Constrained modeling of domain patterns in rhombohedral ferroelectrics

Y. C. Shu,[1,a)] J. H. Yen,[1] H. Z. Chen,[1] J. Y. Li,[2] and L. J. Li[2]
[1]*Institute of Applied Mechanics, National Taiwan University, Taipei 106, Taiwan*
[2]*Department of Mechanical Engineering, University of Washington, Seattle, Washington 98195-2600, USA*

(Received 11 January 2008; accepted 21 January 2008; published online 8 February 2008)

A nonconventional phase-field model is developed to predict ferroelectric domain structures. It employs a set of field variables motivated by multirank laminates to represent energy-minimizing domain configurations, giving rise to an explicit expression of the energy-well structure. The framework is applied to domain simulation in the rhombohedral phase assuming that polarization is close to the ground states. An electromechanical self-accommodation pattern consisting of eight rhombohedral variants and an engineered domain configuration are predicted and found in good agreement with those observed in experiment. © *2008 American Institute of Physics*. [DOI: 10.1063/1.2842385]

Ferroelectric crystals are nonpolar above the Curie temperature but exhibit a number of symmetry-related, spontaneously polarized, and distorted variants below this temperature. Different variants often coexist as domains in very characteristic and intricate patterns.[1] Domains can be manipulated under an external electric field or mechanical load, giving rise to unusual extrinsic or intrinsic electromechanical response in these materials. For example, large electrostrictive actuation can be achieved through non-180° domain switching.[2–5] The intrinsic piezoelectricity, on the other hand, can be enhanced by poling along a nonpolar axis, giving rise to the coexistence of energetically favorable variants.[6–8] Thus, the key to achieving the exceptional potential of ferroelectric materials is to design devices that can take advantage of the inherent domain structures. This, in turn, spurs many scientific efforts for fundamental understanding of domain patterns and their evolution, and calls for computational models suitable for domain simulation. However, much work has addressed the simulation of domain patterns in the tetragonal phase,[9–14] while little has considered the rhombohedral phase,[15] despite unusual properties observed in several relaxor based rhombohedral ferroelectric crystals.[6] This is partly due to the fact that the coefficients of the Landau energy are not readily available for the rhombohedral phase. We describe a nonconventional phase-field approach originally developed for martensite[16] that avoids this difficulty, and report the application of this framework to the prediction of domain patterns of rhombohedral ferroelectrics in this letter.

Consider a ferroelectric single crystal described by two state variables: strain $\boldsymbol{\varepsilon}$ and polarization $\mathbf{p}$. The transformation from the paraelectric to the ith variant of ferroelectric is described by the pair of transformation strain and polarization $(\boldsymbol{\varepsilon}^{(i)}, \mathbf{p}^{(i)})$, and $i=1,\ldots,N$, where N is the number of ferroelectric variants. For rhombohedral ferroelectrics, $N=8$, and we use $r^{(1)}=[111]_c$, $r^{(2)}=[\bar{1}\bar{1}\bar{1}]_c$, $r^{(3)}=[\bar{1}11]_c$, $r^{(4)}=[1\bar{1}\bar{1}]_c$, $r^{(5)}=[1\bar{1}1]_c$, $r^{(6)}=[\bar{1}1\bar{1}]_c$, $r^{(7)}=[11\bar{1}]_c$, and $r^{(8)}=[\bar{1}\bar{1}1]_c$ to label each polarized state. In addition, the transformation strain of the ith rhombohedral variant can be expressed as

$$\boldsymbol{\varepsilon}^{(i)} = 3\delta\hat{\mathbf{r}}^{(i)} \otimes \hat{\mathbf{r}}^{(i)} + (\alpha - \delta)\mathbf{I}, \tag{1}$$

where α and δ are material parameters, $\hat{\mathbf{r}}^{(i)}$ is a unit vector along one of the eight pseudocubic $\langle 111\rangle_c$ crystallographic directions, and $\mathbf{I}$ is the identity tensor. Above the symbol $\mathbf{a}\otimes\mathbf{b}$ denotes the tensor product of two vectors $\mathbf{a}$ and $\mathbf{b}$.

Let $(\boldsymbol{\varepsilon}^*, \mathbf{p}^*)$ be the overall strain and polarization of the crystal. It has been shown that a minimum energy configuration of domains which accommodate these prescribed averages can be coherently constructed by a mixture of ferroelectric variants if all the variants are pairwise electromechanically compatible.[17] Moreover, $(\boldsymbol{\varepsilon}^*, \mathbf{p}^*)$ can be achieved by a rank-$(N-1)$ laminated domain pattern with

$$\boldsymbol{\varepsilon}^* = \sum_{i=1}^{N} \gamma_i \boldsymbol{\varepsilon}^{(i)}, \quad \mathbf{p}^* = \sum_{i=1}^{N} \gamma_i \mathbf{p}^{(i)}, \tag{2}$$

and

$$\begin{aligned} &\gamma_1 = \mu_1, \\ &\gamma_2 = (1-\mu_1)\mu_2, \\ &\cdots \\ &\gamma_{N-1} = (1-\mu_1)\cdots(1-\mu_{N-2})\mu_{N-1}, \\ &\gamma_N = (1-\mu_1)\cdots(1-\mu_{N-2})(1-\mu_{N-1}). \end{aligned} \tag{3}$$

Above, γ_i is the overall volume fraction of the ith ferroelectric variant and μ_i is the local volume fraction of the ith-rank laminate (see, for example, Fig. 1 therein[3]). On the other hand, $(\boldsymbol{\varepsilon}^*, \mathbf{p}^*)$ can also represent the locally inhomogeneous transformation strain and polarization fields if $[\boldsymbol{\varepsilon}^*(\mathbf{x}), \mathbf{p}^*(\mathbf{x})] = (\boldsymbol{\varepsilon}^{(i)}, \mathbf{p}^{(i)})$ for some variant i at each material point $\mathbf{x}$. Motivated by the coherent construction of multirank laminated microstructure, Shu and Yen[16] have suggested to describe the nonuniform transformation fields $[\boldsymbol{\varepsilon}^*(\mathbf{x}), \mathbf{p}^*(\mathbf{x})]$ by μ_i in Eq. (3) restricted to be either 0 or 1 at each point $\mathbf{x}$, which we will adopt here.

Introducing $\boldsymbol{\mu}$ as field variables in addition to $\mathbf{p}$ suggests that the total energy of a ferroelectric crystal, with a slight modification of that proposed by Shu and Bhattacharya,[1] is

[a)]Author to whom correspondence should be addressed. Electronic mail: yichung@spring.iam.ntu.edu.tw.

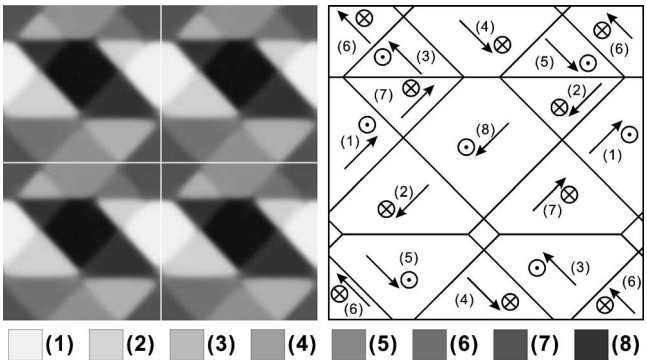

FIG. 1. An electromechanical self-accommodation pattern in the rhombohedral ferroelectric phase. The symbol ⊙ (⊗) denotes the direction of polarization flowing out of (into) the $(001)_c$ surface. Notice that four identical patterns are packed together to obtain a better image.

$$\mathcal{I}(\boldsymbol{\mu},\mathbf{p}) = \int [W^i(\nabla\boldsymbol{\mu},\nabla\mathbf{p}) + W^a(\boldsymbol{\mu}) + W^s(\boldsymbol{\mu},\mathbf{p}) - \boldsymbol{\sigma}^0 \cdot \boldsymbol{\varepsilon} - \mathbf{E}^0 \cdot \mathbf{p}]d\mathbf{x} + \frac{\epsilon_0}{2}\int_{\mathbb{R}^3} |\nabla\phi|^2 d\mathbf{x}, \tag{4}$$

where $\boldsymbol{\sigma}^0$ and $\mathbf{E}^0$ are the applied stress and electric field, ϵ_0 the permittivity of free space, and

$$W^i = A_1|\nabla\boldsymbol{\mu}|^2 + A_2|\nabla\mathbf{p}|^2,$$

$$W^a = K\sum_{i=1}^{N-1} \mu_i^2(1-\mu_i)^2, \tag{5}$$

$$W^s = \frac{1}{2}[\boldsymbol{\varepsilon} - \boldsymbol{\varepsilon}^*(\boldsymbol{\mu})] \cdot \mathbf{C}[\boldsymbol{\varepsilon} - \boldsymbol{\varepsilon}^*(\boldsymbol{\mu})] - [\mathbf{p} - \mathbf{p}^*(\boldsymbol{\mu})] \cdot \mathbf{j}[\boldsymbol{\varepsilon} - \boldsymbol{\varepsilon}^*(\boldsymbol{\mu})] + \frac{1}{2}[\mathbf{p} - \mathbf{p}^*(\boldsymbol{\mu})] \cdot \boldsymbol{\chi}^{-1}[\mathbf{p} - \mathbf{p}^*(\boldsymbol{\mu})].$$

In these equations, W^i with $A_1 > 0$ and $A_2 > 0$ penalizes the changes in the field variables $\boldsymbol{\mu}$ and $\mathbf{p}$, and thus, is interpreted as the energetic cost of forming elastic and polar walls separating different variants. W^a with $K > 0$ is the anisotropy energy density describing the excess of energy when the field variables deviate from the ground states. The third term W^s is the stored energy density with $\mathbf{C}$ as the elastic modulus, $\mathbf{j}$ as the piezoelectric modulus, and $\boldsymbol{\chi}$ as the dielectric susceptibility. The fourth and the fifth terms are the potential energies due to the applied field $\mathbf{E}^0$ and stress $\boldsymbol{\sigma}^0$. The second integral in Eq. (4) is the depolarization energy associated with the electric field generated by the polarization of the crystal itself. Note that the strain field $\boldsymbol{\varepsilon}$ and the depolarization field $\mathbf{E}^d = -\nabla\phi$ are obtained by solving the mechanical equilibrium equation[18] and the Maxwell equation[1] subject to some appropriate mechanical and electrical boundary conditions.

Further simplification can be made if the energy-well structure of $(W^a + W^s)$ is assumed to be steep away from the ground states. This is the constrained assumption commonly adopted in many active materials,[19–21] leading to $\mathbf{p}(\mathbf{x}) = \mathbf{p}^*[\boldsymbol{\mu}(\mathbf{x})]$ for most points of the material. Under this circumstance, the evolution of ferroelectric domains is postulated to be governed by the gradient flow associated with the modified free energy $\mathcal{I}_c(\boldsymbol{\mu}) = \mathcal{I}(\boldsymbol{\mu},\mathbf{p}^*)$ in Eq. (4). This gives

$$\frac{\partial\boldsymbol{\mu}}{\partial t} = -L\frac{\delta\mathcal{I}_c}{\delta\boldsymbol{\mu}} = L\{\mathbf{F}_c^i + \mathbf{F}_c^a + \mathbf{F}_c^e + \mathbf{F}_c^0 + \mathbf{F}_c^d\}, \tag{6}$$

where $L > 0$ is the mobility coefficient, $\mathbf{F}_c^i = 2A_1\nabla^2\boldsymbol{\mu}$ the driving force for coarsening domains, $\mathbf{F}_c^a = -\partial W^a/\partial\boldsymbol{\mu}$ the driving force for selecting variants, $\mathbf{F}_c^e = \mathbf{C}[\boldsymbol{\varepsilon} - \boldsymbol{\varepsilon}^*(\boldsymbol{\mu})] \cdot \partial\boldsymbol{\varepsilon}^*(\boldsymbol{\mu})/\partial\boldsymbol{\mu}$ the driving force for refining elastic domains to accommodate the prescribed boundary conditions, $\mathbf{F}_c^0 = \mathbf{E}^0 \cdot \partial\mathbf{p}^*(\boldsymbol{\mu})/\partial\boldsymbol{\mu}$ the driving force for aligning polarization along the direction of $\mathbf{E}^0$, and $\mathbf{F}_c^d = \mathbf{E}^d \cdot \partial\mathbf{p}^*(\boldsymbol{\mu})/\partial\boldsymbol{\mu}$ the driving force for refining polar domains to reduce the depolarization field $\mathbf{E}^d$.

The present framework is different from the conventional phase-field model[9] from the point of view of energy-well structure. Traditionally, polarization vectors are chosen as the primary order parameters and a special polynomial expansion of them at high orders is required to describe the well structure of energy in the strain-polarization space. Thus, it needs a number of fitting parameters. Instead, a set of field variables $\boldsymbol{\mu}$ motivated by the hierarchical structure of multirank laminates is employed to represent each variant here. It provides an advantage of explicitly expressing the well structure of $(W^a + W^s)$ in Eq. (4), leading to only one parameter K in Eq. (6).

Consider a model example of rhombohedral domain simulation. The material parameters used here are $\alpha = 0$ and $\delta = 0.00131$ in Eq. (1), $P_s = 0.19\ \mathrm{C\,m^{-2}}$, and cubic elastic moduli $C_{11} = 194$ GPa, $C_{12} = 112$ GPa, and $C_{44} = 80$ GPa (Voigt notation) in Eq. (6). The piezoelectric constants are unnecessary due to the constrained assumption $\mathbf{p} = \mathbf{p}^*(\boldsymbol{\mu})$ in Eq. (5), while the dielectric effect is considered by replacing ϵ_0 with $\epsilon_0\kappa$ in the Maxwell equation,[12,22] where κ is the relative dielectric permittivity. Typical values of κ for common ferroelectrics range from hundreds to thousands depending on materials, and $\kappa = 1336$ is taken here. The present formulation involves two additional parameters. The first one is grouped to a dimensionless parameter $D = A_1/K/l_0^2$ where l_0 is the size of the simulation. We take $D = 0.0001$.[16] The other parameter K is chosen such that the energy densities W^a and W^s are of the same order. In addition, the periodic boundary conditions are taken here.

Figure 1 shows a domain pattern under the mechanically clamped boundary condition, where the different variants are presented by different gray levels. Depolarization fields along three $\langle 100\rangle_c$ crystallographical directions are considered in the simulation. The right of Fig. 1 depicts the flow of polarization projected on the $(001)_c$ surface. All of the eight variants coexist forming a mechanically and electrically compatible pattern. Indeed, Fig. 1 shows that the pairs of variants $r^{(1)}/r^{(2)}$, $r^{(3)}/r^{(4)}$, $r^{(5)}/r^{(6)}$, and $r^{(7)}/r^{(8)}$ form 180° domain walls. Moreover, $r^{(1)}/r^{(7)}$ and $r^{(2)}/r^{(8)}$ form 109° domain walls of the type $(110)_c$, and $r^{(3)}/r^{(6)}$ and $r^{(4)}/r^{(5)}$ form another 109° domain walls of the type $(1\bar{1}0)_c$. There are also 71° domain walls of the type $(010)_c$ which separate variants $r^{(1)}/r^{(6)}$, $r^{(2)}/r^{(5)}$, $r^{(3)}/r^{(7)}$, and $r^{(4)}/r^{(8)}$. Besides, it is found that all of these eight variants take nearly equal volume fraction, giving rise to zero overall strain and polarization.

Figure 2 shows a domain pattern under an electric field applied in the nonpolar $[100]_c$ direction, mimicking typical

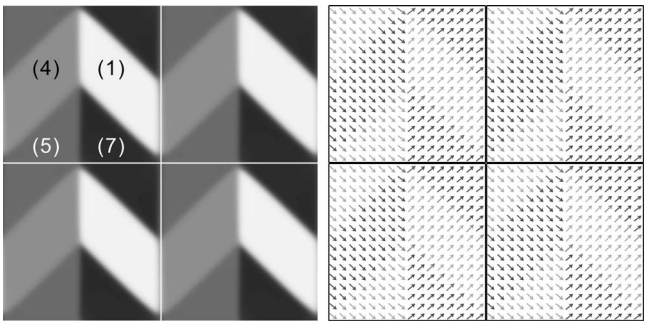

FIG. 2. A rhombohedral domain pattern under an external electric field applied in the nonpolar $[100]_c$ direction. The elastic domain (left) exhibits a herringbonelike structure, while the polar domain (right) exhibits a tire-track pattern.

poling condition for rhombohedral relaxor crystals.[6] Minimizing the term $(-\mathbf{E}^0 \cdot \mathbf{p})$ in Eq. (4) suggests that $r^{(1)}$, $r^{(4)}$, $r^{(5)}$ and $r^{(7)}$ are energetically favorable rhombohedral variants of this case. The elastic domain shown in the left of Fig. 2 is a "herringbonelike" pattern commonly observed in etched samples: long bands traversed by zigzag lines.[23] The flow of polarization is shown on the right of Fig. 2 exhibiting a "tire-track" pattern. This domain configuration has been recently observed in a rhombohedral $Pb(Mg_{1/3}Nb_{2/3})O_3-PbTiO_3$ (PMN-PT) crystal where the etched sample exhibits periodic prominence and depression corresponding to the upward and downward polar directions.[24] Moreover, Liu and Li[8] have attributed the enhanced piezoelectricity found in rhombohedral PMN-PT crystals to crystalline anisotropy, and used this engineered domain pattern to support the argument by finding its effective electromechanical moduli which are one order of magnitude higher than those of a single domain state. This, in turn, raises fundamental issues about how to determine the optimal engineered domains for maximizing piezoelectric response, as well as how to find out suitable electromechanical loadings to generate such optimal domain patterns. These issues are currently under investigation by employing the proposed constrained model.

In summary, a nonconventional phase-field model motivated by energy-minimizing multirank laminates is developed and applied to the prediction of rhombohedral domain patterns. An electromechanical self-accommodation pattern and an engineered domain configuration are predicted, agreeing well with experimental observations.

We are glad to acknowledge the financial support under Grant No. TW NSC (96-2221-E-002-014). J.Y.L. and L.J.L. also acknowledge support from U.S. ARO (W911NF-07-1-0410) and AFOSR (FA9550-07-1-0175).

[1] Y. C. Shu and K. Bhattacharya, Philos. Mag. B **81**, 2021 (2001).
[2] E. Burcsu, G. Ravichandran, and K. Bhattacharya, Appl. Phys. Lett. **77**, 1698 (2000).
[3] Y. C. Shu, J. H. Yen, J. Shieh, and J. H. Yeh, Appl. Phys. Lett. **90**, 172902 (2007).
[4] J. Shieh, J. H. Yeh, Y. C. Shu, and J. H. Yen, Appl. Phys. Lett. **91**, 062901 (2007).
[5] Y. M. Liu, F. X. Li, and D. N. Fang, Appl. Phys. Lett. **90**, 032905 (2007).
[6] S. E. Park and T. R. Shrout, J. Appl. Phys. **82**, 1804 (1997).
[7] S. E. Park, S. Wada, L. E. Cross, and T. R. Shrout, J. Appl. Phys. **86**, 2746 (1999).
[8] D. Liu and J. Y. Li, Appl. Phys. Lett. **84**, 3930 (2004).
[9] L. Q. Chen, Annu. Rev. Mater. Res. **32**, 113 (2002).
[10] J. Slutsker, A. Artemev, and A. L. Roytburd, J. Appl. Phys. **91**, 9049 (2002).
[11] R. Ahluwalia, T. Lookman, A. Saxena, and W. Cao, Appl. Phys. Lett. **84**, 3450 (2004).
[12] S. Choudhury, Y. L. Li, C. E. Krill, III, and L. Q. Chen, Acta Mater. **53**, 5313 (2005).
[13] K. Dayal and K. Bhattacharya, Acta Mater. **55**, 1907 (2007).
[14] Y. Su and C. M. Landis, J. Mech. Phys. Solids **55**, 280 (2007).
[15] T. Liu and C. S. Lynch, *Proceedings of IMECE2006-14945* (ASME, New York, 2006).
[16] Y. C. Shu and J. H. Yen, Appl. Phys. Lett. **91**, 021908 (2007).
[17] J. Y. Li and D. Liu, J. Mech. Phys. Solids **52**, 1719 (2004).
[18] Y. C. Shu, M. P. Lin, and K. C. Wu, Mech. Mater. **36**, 975 (2004).
[19] R. D. James, J. Mech. Phys. Solids **34**, 359 (1986).
[20] A. DeSimone and R. D. James, J. Mech. Phys. Solids **50**, 283 (2002).
[21] Y. F. Ma and J. Y. Li, Acta Mater. **55**, 3261 (2007).
[22] J. Wang and T. Y. Zhang, Appl. Phys. Lett. **88**, 182904 (2006).
[23] J. Ricote, R. W. Whatmore, and D. J. Barber, J. Phys.: Condens. Matter **12**, 323 (2000).
[24] M. C. Shin, S. J. Chung, S. G. Lee, and R. S. Feigelson, J. Cryst. Growth **263**, 412 (2004).